Passive Means for Stabilizing Projectiles with Partially Restrained Internal Members

Albert E. Hodapp Jr.*
Sandia National Laboratories, Albuquerque, New Mexico

A theory is developed to investigate offsetting the center of gravity (*cg*) of a partially restrained internal member (PRIM) from the projectile spin axis to provide a passive means for eliminating the PRIM-induced instabilities that sometimes cause large losses in range and deflection. Results for cylindrical PRIM geometries indicate that, except for large-diameter thin PRIM shapes, small PRIM *cg* offsets, including some that occur randomly within manufacturing tolerances, should be sufficient to reduce the instability-induced range and deflection losses to acceptable levels. Experimental results are presented to confirm the stabilizing effect of PRIM *cg* offset.

Nomenclature

cg = center of gravity
d = body diameter (reference length)
F_T = magnitude of the complex PRIM *cg* offset-generated centrifugal force, Eq. (6)
F_X, F_Y, F_Z = aerodynamic forces acting on body 1 along X, Y, Z axes (Fig. 2), respectively
$F_{X_p}, F_{Y_p}, F_{Z_p}$ = forces acting on the PRIM along X, Y, Z axes (Fig. 2), respectively
i = $(-1)^{1/2}$
I_X, I_Y, I_Z = combined body 1 and PRIM moments of inertia about X, Y, Z axes (Fig. 2), respectively
$I_{X_1}, I_{Y_1}, I_{Z_1}$ = body 1 moments of inertia about X_1, Y_1, Z_1 axes (Fig. 2), respectively
$I_{X_p}, I_{Y_p}, I_{Z_p}$ = PRIM moments of inertia about X_2, Y_2, Z_2 axes (Fig. 2), respectively
I, I_1, I_p = symmetrical equivalents for lateral moments of inertia, $I = I_Y = I_Z$, $I_1 = I_{Y_1} = I_{Z_1}$, $I_p = I_{Y_p} = I_{Z_p}$
K_1, K_2 = respective magnitudes of the complex angle-of-attack slow- and fast-frequency components, Eq. (4)
l_p = PRIM length (Fig. 2)
m, m_1, m_p = combined mass, mass of body 1, and PRIM mass, respectively
M_T = magnitude of the complex PRIM driving moment, Eq. (7)
$M_{X_p}, M_{Y_p}, M_{Z_p}$ = moments acting on the PRIM along X, Y, Z axes (Fig. 2), respectively
p, q, r = roll, pitch, and yaw rates of the combined bodies about X, Y, Z axes, respectively
q' = dynamic pressure, $\rho V^2/2$
r_i, r_o = respective inner and outer radii of a cylindrical PRIM (Fig. 2)
r_T = magnitude of the complex lateral PRIM *cg* offset, Eq. (6)
r_s = stabilizing value of PRIM *cg* offset r_T, Eq. (13)
R_T = torque ratio, Eq. (11), T_T/M_T
S = reference area, $\pi d^2/4$
t = time
T_T = magnitude of the complex PRIM *cg* offset-generated stabilizing torque, Eq. (8)
V = projectile velocity
x_{cg}, y_{cg}, z_{cg} = distances from cg_2 (Fig. 2) to the *cg* of the combined bodies along X, Y, Z axes, respectively
x_1, y_1, z_1 = distances between cg_2 and cg_1 (Fig. 2) along X, Y, Z axes, respectively
X, Y, Z = reference coordinates (Fig. 2)
X_1, Y_1, Z_1 = coordinates fixed in body 1 with X_1 being the axis of geometric symmetry (Fig. 2)
X_2, Y_2, Z_2 = coordinates fixed in the PRIM with X_2 being the axis of geometric symmetry (Fig. 2)
γ = PRIM cant angle (Fig. 1)
γ_0 = destabilizing Fourier component of the PRIM *cg* offset induced γ motion (Fig. 3)
δ_1, δ_2 = respective phase angles of the complex angle-of-attack slow- and fast-frequency components, Eq. (4)
ρ = air density
ϕ = angular displacement of $\tilde{M}_T$ from $\tilde{T}_T$ in the Y-Z plane
$\Delta\phi$ = angular portion of a ϕ quarter-cycle, where $\gamma = 0$
ϕ_γ = angle between the γ and K_1 planes (Fig. 1)
ω_1, ω_2 = contributions to the body-fixed complex angle-of-attack slow and fast frequencies, respectively, Eqs. (4) and (5)
ψ, θ = respective angular displacements of the PRIM-gyroscope test apparatus about the outer and inner gimbals (Fig. 5)
$(\tilde{\ })$ = ( ) is a complex quantity
$(\dot{\ })$ = the derivative of ( ) with respect to time
$()_{max,min}$ = ( ) is a maximum, minimum value, respectively

Introduction

A PARTIALLY restrained internal number (PRIM), one that spins with the surrounding projectile which limited freedom to cant relative to the projectile longitudinal axis of

Presented as Paper 87-2431 at the AIAA Atmospheric Flight Mechanics Conference, Monterey, CA, Aug. 17–19, 1987; received Sept. 8, 1987; revision received Jan. 4, 1988.

*Distinguished Member of the Technical Staff, Aerodynamics Department. Associate Fellow AIAA.

symmetry, has been identified by Vaughn,† Soper,[1] and Murphy[2] as a source for a self-excited resonance-induced instability (diverging angular motion coupled with rapid despin) that has the potential for causing large reductions in range and deflection. As indicated by Fig. 1, the cant angle γ plane (resulting principal-axis misalignment plane) is driven by the angular motion to follow the plane of the K_1 component of complex angle of attack with a phase difference ϕ_γ. Cornell,[3] Morgan,[4] and D'Amico[5] have used recent experimental results to demonstrate that PRIM gyrodynamic motions can reduce the effective cant angle to provide a significant stabilizing effect for certain PRIM geometries. The focus of this article is another important stabilizing effect, one provided by a small body-fixed offset of the PRIM center of gravity (*cg*) from the projectile spin axis.

A theoretical development is presented here to demonstrate that the *cg* offset-induced centrifugal force acting on the PRIM causes additional PRIM motions that reduce PRIM-induced instability by further reducing the effective cant angle. Large longitudinal separations of the PRIM and projectile centers of gravity are not considered in this paper. Therefore, canting, not the motion of the PRIM *cg* about the spin axis (Ref. 2), is the source of instability. Excluding large-diameter thin PRIM shapes, results presented here indicate that small PRIM *cg* offsets, including certain random offsets that occur within manufacturing tolerances, can provide a means for eliminating PRIM-induced instability when other more direct methods such as rigid attachment, spring loading, etc. become impractical. Experimental data, obtained from a laboratory test of limited scope, are presented to confirm the stabilizing effect of PRIM *cg* offset.

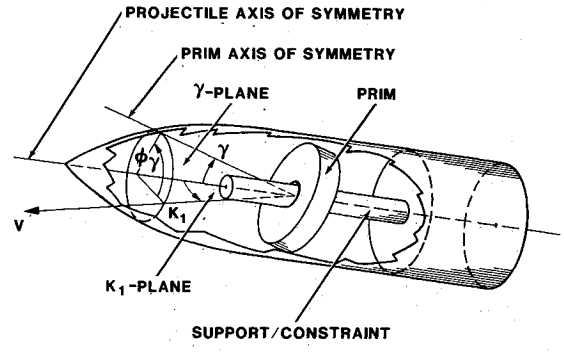

Fig. 1 Projectile with partially restrained internal member (PRIM).

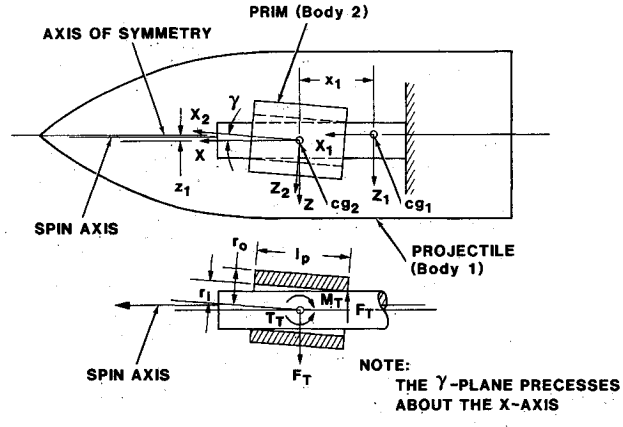

Fig. 2 Coordinate systems, geometry, forces, and moments.

Theoretical Analysis

In Fig. 2, body 1 represents the surrounding projectile and body 2 the PRIM. $X_1Y_1Z_1$ and $X_2Y_2Z_2$ are coordinate systems fixed, respectively, in bodies 1 and 2 with their origins at the respective *cg* locations. In addition to being axes of symmetry for their respective bodies, X_1 and X_2 are assumed to be principal axes. The reference coordinate system $X\ Y\ Z$ has its origin fixed at the *cg* of the PRIM (body 2). X, Y, and Z are parallel with X_1, Y_1, and Z_1, respectively. X is displaced from X_1 to provide the PRIM *cg* offset. The projectile and PRIM (bodies 1 and 2) are constrained to spin together. The PRIM is partially restrained because it can cant about its *cg* through a small angle γ in any lateral plane through the X axis (Fig. 2). $\gamma_{max} = 2\varepsilon/l_p$, where l_p is the PRIM length and ε the radial clearance between the PRIM and its support/constraint (Fig. 2). Radial motion of the PRIM is ignored.

The instabilities that result from the self-excited resonances are caused by extremely small values of γ_{max}. Using the equations of motion for multiple-body systems given in Ref. 6, assume that $\gamma_{max} \leq 0.006$ rad, ignore the contributions to angular momentum from these small canting motions, and replace the subscript 2 of Ref. 6 with a p for PRIM, the vector expressions relative to $X\ Y\ Z$ for the force $\boldsymbol{F}_p$ and moment $\boldsymbol{M}_p$ about cg_2 (Fig. 2) acting on the PRIM become

$$\boldsymbol{F}_p = m_p\left[\frac{\boldsymbol{F}}{m} - \dot{\boldsymbol{\Omega}} \times \boldsymbol{r}_{cg} - \boldsymbol{\Omega} \times (\boldsymbol{\Omega} \times \boldsymbol{r}_{cg})\right] \tag{1}$$

$$\boldsymbol{M}_p = \dot{\boldsymbol{H}}_p + \boldsymbol{\Omega} \times \boldsymbol{H}_p \tag{2}$$

where

$$\boldsymbol{F} = (F_X, F_Y, F_Z)$$

$$\boldsymbol{F}_p = (F_{X_p}, F_{Y_p}, F_{Z_p})$$

$$\boldsymbol{H}_p \approx (I_{X_p}p, I_p q, I_p r)$$

$$\boldsymbol{M}_p = (M_{X_p}, M_{Y_p}, M_{Z_p})$$

$$\boldsymbol{\Omega} = (p, q, r)$$

$$\boldsymbol{r}_1 = (x_1, y_1, z_1)$$

$$\boldsymbol{r}_{cg} = \frac{m_1 \boldsymbol{r}_1}{m} = (x_{cg}, y_{cg}, z_{cg})$$

$$m = m_1 + m_p$$

The expressions given next are used to write the lateral components of Eqs. (1) and (2) in terms of the modal amplitudes and frequencies of projectile angular motion. These approximations were obtained from a small-angle linear solution for projectile angular motion relative to the $X\ Y\ Z$ body-fixed coordinates (Fig. 2).

$$q + ir \approx -i(\dot{\beta} + i\dot{\alpha}) + p(\beta + i\alpha) \tag{3}$$

$$\beta + i\alpha \approx K_1 e^{i[(\omega_1 - p)t + \delta_1]} + K_2 e^{i[(\omega_2 - p)t + \delta_2]} \tag{4}$$

The angle of attack and side-slip angle are α and β, respectively. $K_{1,2}$ and $\delta_{1,2}$ are real constants that are determined by the initial conditions. The familiar fast and slow frequencies relative to nonrolling coordinates ω_1 and ω_2, respectively, are defined by

$$\omega_{1,2} = \left(\frac{pI_X}{2I}\right)\left[1 \pm \sqrt{1 - 1/S_g}\right] \tag{5}$$

†H. R. Vaughn's contributions are contained in a Sandia National Laboratories publication of limited distribution.

where the gyroscopic stability factor S_g is defined as

$$S_g = \left(\frac{pI_X}{2I}\right)^2 / q'Sd\left[C_{M_\alpha} - C_{N_\alpha}\left(\frac{x_{cg}}{d}\right)\right]/I$$

C_{M_α} and C_{N_α} are the pitching-moment slope and the normal force slope coefficients, respectively, for the symmetrical projectile. The moments of inertia are given approximately as

$$I_X \approx I_{X_1} + I_{X_p}$$

$$I \approx I_1 + I_p + m\left(\frac{m_p}{m_1}\right)x_{cg}^2$$

Small contributions resulting from x_{cg}, lateral aerodynamic force $F_Y + iF_Z$, and gravity have all been neglected in Eq. (3). Through Eq. (4), damping, yaw of repose, and PRIM *cg* offset-induced principal-axis misalignment all have negligible effects on PRIM forces and moments; therefore, they were neglected. Small contributions from products of the small perturbation quantities y_{cg} and z_{cg} have been neglected in the foregoing expressions for moment of inertia.

If we expand Eqs. (1) and (2), assume small angular motions, and substitute Eqs. (3) and (4), the lateral force and moment acting on the PRIM can be reduced to the following approximate complex forms:

$$\tilde{F}_T \approx m_p p^2 \tilde{r}_T \tag{6}$$

$$\tilde{M}_T \approx i(I_p\omega_1 - I_{X_p}p)\omega_1 K_1 e^{i[(\omega_1 - p)t + \delta_1]} \tag{7}$$

where

$$\tilde{F}_T = F_{Y_p} + iF_{Z_p}$$

$$\tilde{M}_T = M_{Y_p} + iM_{Z_p}$$

$$\tilde{r}_T = y_{cg} + iz_{cg}$$

Equation (6) indicates that a small PRIM *cg* offset r_T can provide the dominant contribution to lateral force acting on the PRIM. This reduced form of the PRIM lateral force equation results from assuming that x_{cg} remains small [$x_{cg} < 0.1(r_T/K_1)(I/I_x)^2$] and that contributions from products of the small perturbation quantities q, r, y_{cg}, and z_{cg} are negligible as are contributions from $\dot{p}$ and $F_Y + iF_Z$. Elimination of K_2-dependent terms in Eq. (7) is justified by the fact that $K_1 \approx K_2$ and $\omega_1 \gg \omega_2$ for gun-launched, spin-stabilized projectiles. Experimental results[2-5] confirm that the K_1 component of Eq. (4) provides the dominant contribution to the PRIM driving moment $\tilde{M}_T$.

As indicated by Fig. 2, the centrifugal force $\tilde{F}_T$ acting laterally through the PRIM *cg* produces a moment $\tilde{T}_T$ that always opposes $\tilde{M}_T$. Therefore, an expression for $\tilde{T}_T$ is obtained by multiplying $\tilde{F}_T$, Eq. (6), by the moment arm $il_p/2$.

$$\tilde{T}_T \approx \pm im_p l_p p^2 \tilde{r}_T/2 \tag{8}$$

The $\pm$ sign indicates that this body-fixed moment changes direction by 180 deg to oppose $\tilde{M}_T$.

In comparing Eqs. (7) and (8), note that the moment $\tilde{M}_T$ rotates in the Y-Z plane (Fig. 2) relative to $\tilde{T}_T$ at the rate $\dot{\phi} = \omega_1 - p$. As illustrated in Fig. 3, PRIM canting is eliminated ($\gamma = 0$) over portions of a ϕ cycle when

$$|\tilde{T}_T \cos\phi| > |\tilde{M}_T| \tag{9}$$

The PRIM gyrodynamic motions described in Ref. 3 have been omitted in Fig. 3 to clarify the effect of $\tilde{T}_T$. The minimum value of ϕ that satisfies Eq. (9) also defines the $\Delta\phi$ portion of the first and each successive quarter-cycle, where $\gamma = 0$ (Fig. 3).

$$\Delta\phi = \arccos(1/R_T) \tag{10}$$

$$R_T = T_T/M_T \tag{11}$$

Note that $\Delta\phi$ is defined for $1 \le R_T < \infty$, that is, only when $\tilde{T}_T$ is greater than, or equal in magnitude to, $\tilde{M}_T$.

A Fourier analysis of the forcing-function amplitude (Fig. 3) has revealed that the amplitude γ_0 of the destabilizing component can be reduced to zero as $R_T \to \infty[\Delta\phi \to \pi/2$, Eq. (10)].

$$\frac{\gamma_0}{\gamma_{\max}} = 1 - \frac{2}{\pi}\arccos(1/R_T) \tag{12}$$

Note that Eq. (12) represents the average or effective value of the cant angle γ (Fig. 3). Therefore, PRIM *cg* offset $\tilde{r}_T$ provides a means to reduce or eliminate the destabilizing effects of the PRIM when its magnitude r_T becomes large enough to make $R_T > 1.0$. These stabilizing values of PRIM *cg* offset are denoted by r_S. An expression for stabilizing offset is obtained by substituting Eqs. (7) and (8) into Eq. (11), which results in Eq. (13).

$$r_S \approx 2K_1R_T\left(\frac{\omega_1}{p}\right)\left(\frac{I_{X_p}}{m_p l_p}\right)\left[1 - \left(\frac{I_p}{I_{X_p}}\right)\left(\frac{\omega_1}{p}\right)\right], \quad R_T > 1.0 \tag{13}$$

Results and Discussion

Equation (13) obscures the dependence of stabilizing offset r_s on roll rate p, PRIM size, PRIM shape, and projectile mass properties. The gyroscopic stability factor S_g, Eq. (5), is usually sufficiently large for ω_1/p to be approximated by $I_x/I[S_g > 3.0$, Eq. (5)]. This approximation and an assumed cylindrical PRIM geometry are used to reduce Eq. (13) to

$$r_S \approx \frac{r_o^2}{l_p}\left(\frac{I_X}{I}\right)\left\{\left[1 + \left(\frac{r_i}{r_o}\right)^2\right]\left[\frac{1}{2}\left(\frac{I_X}{I}\right) - 1\right] + \frac{1}{6}\left(\frac{l_p}{r_o}\right)^2\left(\frac{I_X}{I}\right)\right\}K_1R_T \tag{14}$$

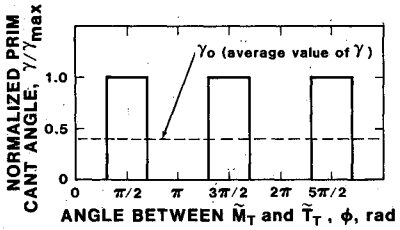

Fig. 3 PRIM cg offset-induced canting motions.

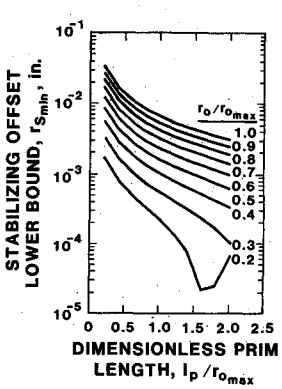

Fig. 4 Effect of PRIM radius and length on the onset of the stabilizing effect for a 155-mm projectile.

where r_i and r_o are the inner and outer PRIM radii, respectively (Fig. 2). Although roll rate p does not appear explicitly in Eq. (14), stabilizing offset is dependent on p through R_T. Recall from Eq. (41) of Ref. 2 that the $\dot{K}_1 > 0$ induced by the PRIM is proportional to p and $\gamma \sin\phi_\gamma$. Results from Refs. 3 and 4 indicate that roll rate-induced changes in $\gamma \sin\phi_\gamma$ are expected to be small. Therefore, for a given projectile/PRIM combination and K_1 level, r_s increases with increasing p because R_T must increase (γ_0/γ_{max} must decrease) to insure stability. Equation (14) reveals that in addition to dependence on the product $K_1 R_T$, r_S is dependent on the projectile moment of inertia ratio I_X/I and PRIM size and shape through r_i, r_o and l_p. Unlike PRIM-induced instability, r_s is independent of PRIM density.

Figure 4 illustrates the effects that PRIM length l_p and outer radius r_o have on the magnitude of the stabilizing offset r_S for a typical 155-mm projectile. If we use $K_1 = 1.0$ deg, $I_X/I = r_i/r_o = 0.1$, and $r_{o_{max}} = 3.05$ in. (77.5 mm), the onset of the stabilizing effect $r_{S_{min}}$ [Eq. (14), $R_T = 1.0$] is plotted vs $l_p/r_{o_{max}}$ for discrete values of $r_o/r_{o_{max}}$. The actual r_S for these conditions will be slightly larger because $r_S > r_{S_{min}}$ is required for stability. Note that $r_{S_{min}}$ remains extremely small except for $r_o/r_{o_{max}}$ approaching 1.0 and for $l_p/r_{o_{max}}$ approaching zero. Under these conditions, the required $r_{S_{min}}$ can become large enough to exceed physical constraints imposed by the projectile. Outside of those narrow bands of $l_p/r_{o_{max}}$ and $r_o/r_{o_{max}}$, the required stabilizing offset r_S should be small enough to provide a usable means for reducing or eliminating PRIM-induced instability.

Experimental verification of the stabilizing effect of PRIM *cg* offset was obtained in the laboratory through the use of the gyroscope apparatus described in Ref. 3 and shown in Fig. 5. The freely gimbaled gyroscope contains a hollow cylindrical PRIM that spins with, and is partially restrained by, a motor-driven central shaft. PRIM spin rate was maintained at a constant value near 60 Hz. Parameters given in Table 1 characterize the gyroscope and PRIM. This experiment was designed to provide results representative of those obtained for the PRIM test projectile (PRIM-TP). Characteristics of the 155-mm PRIM-TP, an internally modified *M*549 developed for a future flight test, are also given in Table 1.

The $\psi - \theta$ angular motions of the PRIM-gyroscope (Fig. 5) were self-excited and unstable ($\dot{K}_1 > 0$) (Ref. 3) when PRIM *cg* offset was absent ($r_T = 0$). When PRIM *cg* offset was present ($r_T > 0$), an external disturbance ($K_1 > 0$) was required to excite the gyroscope into motion. Experimental results (circular symbols) and the $r_{S_{min}}$ line (onset of stabilizing effect) for the gyroscope are presented in Fig. 6, where PRIM *cg* offset r_T is plotted vs initial disturbance K_1. Note that the theoretically predicted stable and unstable regions (separated by the $r_{S_{min}}$ line) contain only stable (open symbol) and unstable (solid symbol) experimental results, respectively. As predicted by Eqs. (13) and (14), the $r_T = 0.007$ in. (0.178 mm) data in Fig. 6 demonstrate that the ability for a fixed offset r_T to provide a stabilizing effect is dependent on the level of K_1. Although $r_T > r_{S_{min}}$ introduces a stabilizing effect, uncertain stability exists over the lower region above $r_{S_{min}}$ because $R_T > 1.0$ is required for stability. Values of R_T for the $K_1 = 3.5$, 6.5, and 11.0 deg stable points in Fig. 6 were 2.43, 2.83, and 1.70, respectively ($\gamma_0/\gamma_{max} = 0.27$, 0.23, and 0.40). The experimental results given in Fig. 6 demonstrate that very small PRIM *cg* offsets can stabilize the otherwise unstable gyroscope (Fig. 5) for large values of K_1.

Flight simulation results are given in Fig. 7 for the PRIM-TP at firing conditions that maximize range loss due to PRIM-induced instability. These results are based on Eq. (13) and Eqs. (41) and (42) of Ref. 2, with an effective $\gamma \sin\phi_\gamma$ equal to 20% of the maximum value, as suggested by Ref. 3. Note that K_1 damps initially because of the strong aerodynamic damping effect that is present at low altitudes. This causes the stabilizing

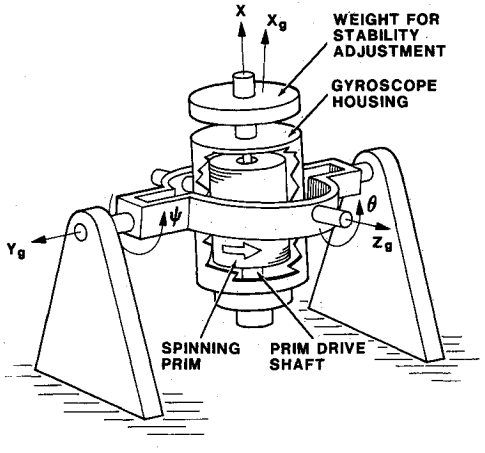

Fig. 5 PRIM-gyroscope test apparatus.

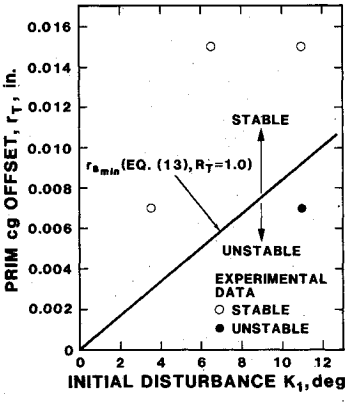

Fig. 6 Experimental confirmation of the stabilizing effect of PRIM cg offset.

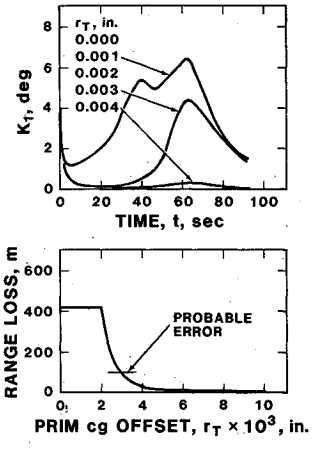

Fig. 7 Simulated stabilizing effects of PRIM cg offset on projectile flight performance.

Table 1 Characteristics of the PRIM-gyroscope test apparatus and PRIM test projectile (PRIM-TP)

Parameter	PRIM-gyroscope	PRIM-TP
I_X/I	0.043	0.080
I_{X_p}/I_p	0.85	0.76
$I_{X_p}/m_p l_p$	0.59 in. (14.9 mm)	0.64 in. (16.3 mm)
m	Not applicable	2.97 slug (43.3 kg)
r_T	0.007 in. (0.18 mm) or 0.015 in. (0.38 mm)	0.015 in. (0.38 mm)
x_{cg}	Approx. 1.0 in. (25.4 mm)	Approx. 0
γ_{max}	0.006 rad (0.34 deg)	0.006 rad (0.34 deg)

offset to be much smaller than the expected value based on the initial magnitude of K_1. An acceptable range loss from PRIM-induced instabilities is one that is small when compared to the expected probable error that characterizes range dispersion for a rigid projectile. The results given in Fig. 7 indicate that levels of r_T smaller than those used to obtain the experimental results (Fig. 6) may be sufficient to reduce range loss from PRIM-induced instabilities to an acceptable level. Small offsets like these can easily fall within the high-probability portion of a distribution of random PRIM *cg* offsets that occur within projectile-manufacturing tolerances. Therefore, a production version of a projectile like the PRIM-TP can be expected to display acceptable range performance for most firings.

Conclusion

It has been demonstrated theoretically that a small offset of the PRIM *cg* from the projectile spin axis can provide an effective means for reducing or eliminating the PRIM-induced instabilities that sometimes cause large reductions in range and deflection. This passive means for stabilization becomes ineffective for large-diameter, thin PRIM shapes because the required offsets can exceed physical constraints imposed by the projectile. Outside of these narrow bands of diameter and thickness, PRIM *cg* offsets as small as some that occur randomly within manufacturing tolerances should provide an effective means for eliminating PRIM-induced instabilities. The stabilizing effect of PRIM *cg* offset was confirmed by experimental results.

Acknowledgments

This work was performed at Sandia National Laboratories, supported by the U.S. Department of Energy under Contract DE-AC04-76DP00789. The author gratefully acknowledges the assistance provided by H. R. Vaughn (retired) of Sandia National Laboratories. Experimental data were provided by T. O. Morgan and R. H. Cornell of the Lawrence Livermore National Laboratory.

References

[1]Soper, W. G., "Projectile Instability Produced by Internal Friction," *AIAA Journal,* Vol. 6, Jan. 1978, pp. 8-11.

[2]Murphy, C. H., "Influence of Moving Internal Parts on Angular Motion of Spinning Projectiles," *Journal of Guidance and Control,* Vol. 1, March-April 1978, pp. 117-122.

[3]Cornell, R. H., "Experimental Investigation of Dynamic Motions of an Internal Part in an Artillery Projectile," AIAA Paper 85-1842, Aug. 1985.

[4]Morgan, T. O., "The Influence of Internal Moving Parts on the Ballistic Flight Path of a Projectile," AIAA Paper 85-1841, Aug. 1985.

[5]D'Amico, W. P., "A Comparison Between Theory and Experiment for the Yaw Moment Induced by a Loose Internal Part," AIAA Paper 85-1826, Aug. 1985.

[6]Hodapp, A. E., Jr., "Equations of Motion for Free-Flight Systems of Rotating-Translating Bodies," Sandia Lab., Albuquerque, NM, SAND 76-0266, 1976.